Input of advanced geotechnical modelling to the design of offshore wind turbine foundations (Apport de la modélisation géotechnique avancée au dimensionnement de fondations d'éoliennes offshore)

Pisano, Federico

DOI
10.32075/17ECSMGE-2019-1099

Publication date
2019

Document Version
Accepted author manuscript

Published in
17th European Conference on Soil Mechanics and Geotechnical Engineering, ECSMGE 2019 - Proceedings

Proceedings of the XVII ECSMGE-2019
Geotechnical Engineering foundation of the future
ISBN 978-9935-9436-1-3

doi: 10.32075/17ECSMGE-2019-1109

XVII European Conference
ECSMGE 2019
Reykjavik
on Soil Mechanics
and Geotechnical Engineering

Input of advanced geotechnical modelling to the design of offshore wind turbine foundations

Apport de la modélisation géotechnique avancée au dimensionnement de fondations d'éoliennes offshore

F. Pisanò

Faculty of Civil Engineering & Geosciences / Delft University of Technology, Delft, The Netherlands

ABSTRACT: The offshore wind sector is skyrocketing worldwide, with a clear trend towards wind farms installed in increasingly deep waters and harsh marine environments. This is posing significant engineering challenges, including those regarding the design of support structures and foundations for offshore wind turbines (OWTs). Substantial research efforts are being devoted to the geotehnical design of monopile foundations, currently supporting about 80% of OWTs in Europe. This paper overviews recent work carried out at TU Delft on the numerical integrated modelling of soil-monopile-OWT systems, and its input to the improvement of geotechnical design approaches. The benefits of incorporating advanced soil constitutive modelling in three-dimensional finite element simulations are highlighted, with emphasis on the interplay of cyclic soil behaviour and dynamic OWT performance. Ongoing research on high-cyclic soil plasticity modelling is also presented, and related to the analysis of monopile tilt under irregular environmental loading.

RÉSUMÉ: Le secteur de l'éolien offshore grimpe en flèche partout dans le monde, avec une tendance claire pour les parcs installés à de plus en plus grandes profondeurs et dans des environnements marins particulièrement compliqués. Ces conditions posent d'importants enjeux d'ingénierie, notamment liés au dimensionnement des structures de support et des fondations des turbines éoliennes offshores (OWTs). Des efforts de recherche significatifs sont consacrés au dimensionnement de fondation pour monopieux, qui supportent près de 80% des OWTs en Europe. Ce papier présente un aperçu des travaux réalisés à TU Delft sur la modélisation numérique intégrée de systèmes sol – monopieux – OWTs. Les bénéfices de modèles constitutifs avancés de sol sont mis en évidence, avec une attention particulière sur les interactions entre le comportement cyclique des sols et la dynamique des OWTs. Les recherches en cours sur la modélisation d'un grand nombre de cycles sont aussi présentées, et associées à l'analyse du basculement de monopieux sous chargement environnemental non-monotone.

Keywords: offshore wind energy; numerical modelling; monopile foundations; cyclic loading; dynamics

1 INTRODUCTION

The gradual depletion of hydrocarbon reserves is shifting the global energy mix towards clean and sustainable sources, with solar and wind energies gradually gaining larger shares. The wind energy sector is skyrocketing worldwide, especially with respect to installations in the ocean. Recent

technological advances have fostered impressive growth in size and power output of offshore wind turbines (OWTs) (Fig. 1), along with remarkable reduction of fabrication and installation costs. To date, Europe remains the main player in offshore wind, with the North Sea hosting most wind farms in the continent (~70%), and the Irish Sea, Baltic Sea and Atlantic Ocean witnessing new developments (WindEurope, 2018). Discussions about extending offshore wind farming to the Mediterranean Sea are also ongoing (Balog et al., 2016).

Owing to extensive research started in the late 1990s, offshore wind technology is nowadays mature in many areas, and constantly looking forward to new challenges. Reportedly, latest offshore wind projects are developing in waters of increasing depth and distance from the shore, as illustrated in Fig. 2 for bottom-fixed wind farms in Europe (WindEurope, 2018). The trend towards "deeper & farther" is instrumental to building wind farms with larger power output, or sometimes simply unavoidable in presence of large water depths close to the shore (Rodrigues et al., 2015). The latter case is relevant, for instance, to recent offshore wind plans in the United States and Japan (Jacobson et al., 2015; Ushiyama, 2018), and has promoted in the last decade considerable studies regarding floating wind farms (Castro-Santos & Diaz-Casas, 2016) – not considered in this paper.

Installations in deeper waters imply harsher environments and loading conditions, and thus serious technical challenges regarding the design of support structures and foundations. Restricting attention to the case of bottom-founded (i.e. non-floating) OWTs, a number of foundation setups have been proposed over the years, including deep and shallow foundations assembled as either single or compound units (Byrne & Houlsby, 2003) (Fig. 3). Discussions about their suitability still take place at most international geo-events, during themed sessions dedicated to the testing, analysis and design of OWT foundation systems – see for instance Pisanò & Gavin (2017).

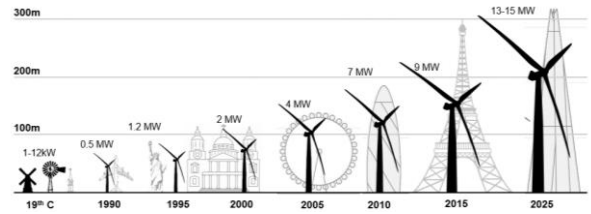

Fig. 1. Evolution of wind turbine size and power output (from Bloomberg New Energy Finance)

About 80% of all OWTs in Europe are founded on monopiles (MPs), tubular steel piles of large diameter (~5-10 m) and embedment ratio (embedded length/diameter) in the range from 3 to 6 (Fig. 4). Bigger OWTs in deeper waters require larger monopiles – expected to reach up to 15 m diameter in the future – depending on site-specific soil conditions and environmental loading from wind and waves. Furthermore, recent developments in south-eastern Asia, e.g. in Taiwan (Zhang et al., 2017), are drawing attention to the design of earthquake-resistant structures and foundations (Kaynia, 2018).

At current state of practice, monopiles of 8-10 m diameter for 30 m water depth can easily require for their fabrication more than 1000 tonnes of steel. As foundation costs still amount

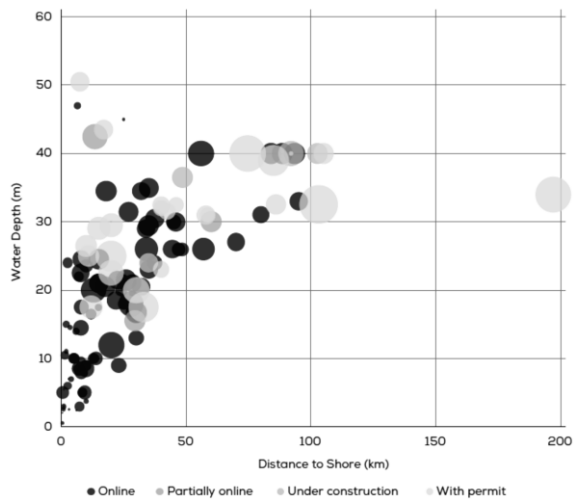

Fig. 2. Water depth and distance to shore of bottom-fixed offshore wind farms, organised by development status (modified after WindEurope, 2018)

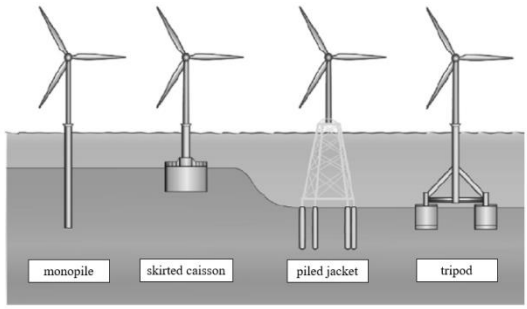

Fig. 3. Most common foundation concepts for bottom-fixed OWTs (modified after Kaynia, 2018)

to 30-40% of the capital expenditure, the industry is strongly driven towards optimisation (Doherty & Gavin, 2011).

The present paper summarises recent TU Delft research regarding OWT foundations and their analysis via advanced numerical modelling. After introducing geotechnical drivers for MP design (Section 2), theory and set-up of 3D finite element (FE) models for OWT-MP-soil systems are overviewed in Section 3, with focus on the case of MPs in sandy soils; Section 4 illustrates how advanced 3D FE modelling can fruitfully serve the non-linear dynamic analysis of OWTs, and provide precious input to improve existing design tools; the open issue of predicting MP tilt under environmental loading is addressed in Section 5, and related to ongoing research on the constitutive modelling of high-cyclic sand behaviour. The main goal of the paper is to point out how advanced numerical modelling can impact the understanding of soil-structure interaction in OWTs, and promote enhanced geotechnical design for further cost-reduction.

Fig. 4. OWT MP at Port of Rotterdam (Netherlands)

2 DESIGN OF MP FOUNDATIONS

Monopile dimensions (length, diameter, wall thickness) must be designed to guarantee safe performance under OWT loads, in presence of surrounding soil reactions (Arany et al., 2017; Bhattacharya, 2019). At present, the main industry guidelines for MP design are those in the DNVGL-ST-0126 document (DNV-GL, 2016), prescribing the following design checks:

1. the first natural frequency of the global OWT-MP-soil system must fall within prescribed limits, and ensure *soft-stiff* behaviour (Fig. 5);
2. MPs must not fail under prolonged loading during the whole OWT operational life (FLS, Fatigue Limit State);
3. MPs must not fail under loads of exceptional magnitude (ULS, Ultimate Limit State);
4. MPs must remain fully usable under ordinary loading, i.e. only limited deformations are allowed (SLS, Serviceability Limit State).

While checks 2-4 underlie usual limit states for offshore structures, check 1 is a peculiar design requirement for OWTs. Undesired resonances are to be avoided by keeping f_0 (global natural frequency associated with the first bending mode) within the f_{1P}-f_{3P} range – f_{1P} is the rotor revolution frequency, while f_{3P} (for three-bladed OWTs) the frequency of the aerodynamic pulses induced by the passage of each blade (*shadowing effect*). Setting $f_{1P} < f_0 < f_{3P}$ is commonly referred to as *soft–stiff* design, as it combines a stiff superstructure with a more compliant foundation.

Checks 1 and 2 are mostly dictated by soil behaviour at small strains, whereas check 3 relates to the non-linear, near-failure regime. Check 4 is transversal to different conditions, though mostly relevant to normal operations.

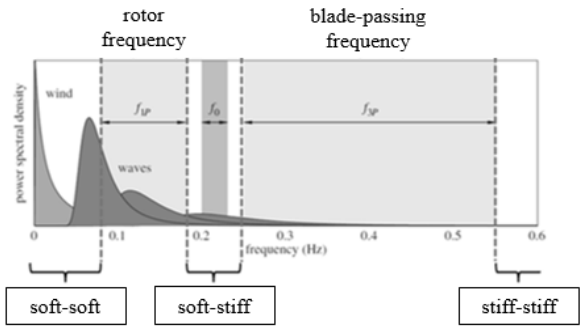

Fig. 5. Excitation ranges in the frequency-domain and design set-ups associated with different OWT and foundation stiffness (modified after Kallehave et al., 2015)

Performing the above design checks is highly challenging in presence of realistic environmental cyclic loading (ECL). ECL is known to mobilise non-trivial aspects of soil behaviour, such as variations in stiffness and strength, energy dissipation, build-up of pore water pressures, and accumulation of permanent deformations (di Prisco and Wood, 2012). For instance, cyclic soil deformations may induce unacceptable monopile tilt (Abadie et al, 2018), a serviceability issue (check 4) that is often mitigated through larger MP embedment depth. Uncertainties about cyclic soil behaviour lead to conservatism in design, i.e. non-optimal use of steel.

MP design for offshore wind projects is commonly performed via *p-y modelling*, i.e. by lumping soil reactions along the MP into distributed spring elements. The DNVGL-ST-0126 document (DNV-GL, 2016) questions the suitability of existing p-y models (e.g. from API, 2014) for stiff piles, and recommends more advanced experimental and numerical studies to "*better assess the possible failure modes, drainage mechanisms, effective stresses and the effects of high- or low-level cyclic loading*". Although the PISA project has recently released new monotonic p-y curves for MPs (Byrne et al., 2019), further work seems still needed for geotechnically sound design of MPs under ECL.

About filling such knowledge gaps, the research agenda by the European Academy of Wind Energy (EAWE) indicates the road for moving offshore wind geotechnics forward (van Kuik et al., 2016). In Section 8 (*Hydrodynamics, soil characteristics and floating turbines*) the Authors observe: ''*What is the amount of soil damping for an offshore turbine? Is it possible to estimate soil damping from first principles, like from numerical simulation with solid elements? Improved insight could lead to major breakthroughs like a possible pile eigenfrequency fine tuning through varying ramming depth as a function of soil characteristics and other key variables*". At a first glance, the EAWE agenda points to the chance of studying soil mechanisms and energy dissipations in OWTs (*damping*) through 3D numerical models (*solid elements*). Ultimately, van Kuik et al. (2016) support the use of advanced numerical analysis as a way to gain deeper insight into governing mechanics, and promote the improvement of design methods.

The EAWE agenda inspired the research thread overviewed herein, about the advanced numerical modelling of OWT foundations.

3 INTEGRATED 3D FE MODELLING OF OWT-MP-SOIL SYSTEMS

This section covers the set-up of integrated 3D FE models of OWTs, including turbine tower, foundation and soil. The developments presented hereafter are aligned with the EAWE research agenda (van Kuik et al., 2019), in an effort to help unveil the role of several geotechnical factors in OWT design. The importance of integrated modelling is nowadays widely acknowldged in relation to complex structural systems, among which bottom-founded offshore structures offer a notable example (Bienen and Cassidy, 2006; Aasen et al., 2017; Pisanò et al., 2019).

The highest level of OWT model integration – i.e. including structure, water, air and soil – is not pursued herein. Emphasis is on building 3D FE models with advanced representation of non-

linear soil behaviour and cyclic/dynamic soil-MP interaction.

3.1 Governing equations and model set-up

Fig. 6a illustrates the idealisation of a MP-supported OWT subjected to wind/wave loading. As full integration of water and air in the modelling is not considered, aero- and hydro-dynamic loads are to be provided as an input, with no two-way interaction between such loads and structural vibrations. Established approaches for determining external loads on OWTs are described in Bhattacharya (2019). In the lack of fluid-structure interaction modelling, water added mass effects (inertial interaction) can be simplistically introduced through water lumped masses, e.g. as proposed by Newman (1977).

The same system in Fig. 6a is presented in its discretised FE version in Fig. 6b, formed by the following components (Corciulo et al., 2017a):

- OWT tower plus the portion of the pile above the mudline modelled as a Timoshenko beam. For realistic OWT modelling, beam elements with mass density and stiffness variable along the elevation are normally used, with the addition of lumped masses for RNA (Rotor-Nacelle Assembly) and equipment (flanges, transition piece, working platforms, etc.) (Kementzetzidis et al., 2019a);
- embedded length of the pile modelled through either 3D solid elements or 2D shells. The use of 1D embedded beams is not recommended, as it would hinder proper representation of 3D soil-MP interaction (e.g. effect of distributed shear stresses, presence of soil plug, bottom shear/moment fixity);
- soil around the foundation represented as a 3D domain discretised via solid elements. Underwater soils are normally water-saturated. They respond to external loading

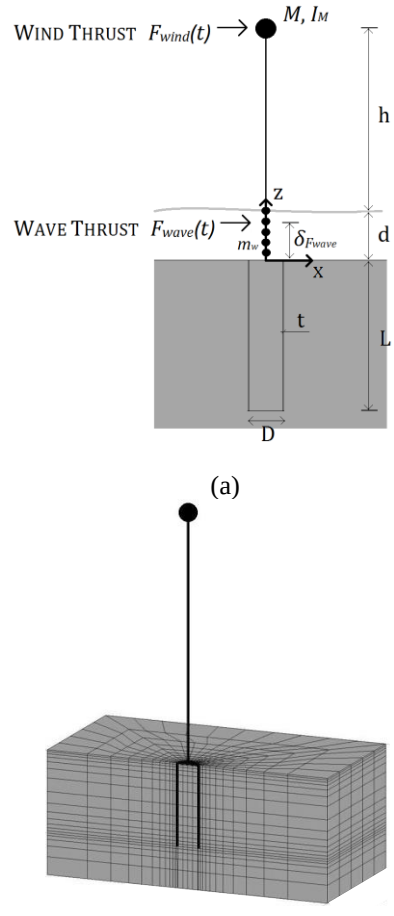

Fig. 6. (a) Idealisation of a MP-supported OWT subjected to wind/wave loading, and (b) associated 3D FE model (modified after Corciulo et al., 2017a)

under drainage conditions that approach the drained or undrained limit depending on their hydraulic/mechanical properties. The dynamic consolidation of saturated soils has been widely studied in the literature after Biot's pioneering work (Biot, 1956a-b). Zienkiewicz et al. (1980) discussed significance and applicability of different mathematical formulations, in relation to the interplay of loading frequency and soil permeability. Based on linear elastic analysis, Ziekiewicz et al. concluded that many problems in earthquake geotechnics – i.e. involving frequencies mostly lower than 10 Hz – can be

tackled through the so-called *u-p formulation* of relevant conservation laws (balance of linear momentum and pore water mass). Based on the assumption of no relative acceleration between pore water and solid skeleton, the u-p formulation is the most economical among all options, as it only requires in 3D domains the determination of three displacement components for the soil ($\boldsymbol{u}$) and a scalar field for the pore pressure (p). Details regarding formulation and numerical solution of dynamic problems in saturated soils can be found in Zienkiewicz et al. (1999); more recent discussions about the suitability of different formulations in two-phase soil dynamics are provided by Jeremić et al. (2008) and Staubach & Machacek (2019). As environmental/mechanical loads on OWTs are rather slow (frequencies lower than 1 Hz, Fig. 4), the use of the u-p formulation in offshore wind problems is not to be questioned.

After space discretisation, the model in Fig. 6a can be used for time-domain simulations under given initial and boundary conditions. To date, dynamic FE models of OWT-MP-soil systems (Fig. 6b) have found only limited application in offshore wind geotechnics, for instance in the works by Cuéllar et al. (2014), Corciulo et al. (2017a), Barari et al. (2017), Kementzetzidis et al. (2019a).

A number of set-up choices can impact the accuracy and computational burden of a 3D FE model of the type in Fig. 6a:

Soil element type. Two-phase soil elements are needed to obtain both displacements and pore pressures in the soil domain. In this respect, it is well-known that only certain types of elements are suitable for hydro-mechanical simulations. To avoid instabilities in the pore pressure field (checker-board modes) under (nearly) undrained conditions, using stabilised elements with linear interpolation for both diplacements and pressures seems the best option. Stabilisation techniques for mixed elements with equal order interpolation have been widely studied for incompressible problems, (Zienkiewicz et al., 1999), as a way to circumvent the so-called LBB condition and minimise the number of degrees-of-freedom in FE models. Recently proposed *H1P1ssp* elements (stabilised single point) elements (McGann et al., 2015) have been exploited to reduce computational burdens in the present thread of work. As explained in the original publication, *H1P1ssp* brick elements do not only remedy undrained pore pressure instabilities, but can also mitigate inaccuracies related to volumetric locking effects;

Boundary conditions. Hydraulic and mechanical boundary conditions must be set along the lateral surface of the 3D soil domain (Fig. 6b). Since neither the mechanical soil response nor the flow of pore water depend on the absolute water depth, it is possible to set nil pore pressure at the mudline. This is a simplification enabled by the assumption of no-interaction between free and interstitial water (Jeng, 2003). Regarding mechanical boundary conditions, it is worth noting that in presence of low-frequency cyclic loading (Fig. 5), typical concerns about absorbing outgoing waves become less relevant. Indeed, since MP vibrations occurr at frequencies usually lower than the so-called *cut-off threshold* (Graff, 1975), no real waves can be generated and propagated through the soil domain – only *evanescent*, spatially decaying waves can exist. As a consequence, static node fixities work properly as long as lateral boundaries are sufficiently far from the structure – in the order of 5-6 pile diameters (Corciulo et al., 2017a, Kementzetzidis et al., 2019a).

Soil-MP interface modelling. Following the approach by Griffiths (1985), the simplest way to model soil-MP interface is to introduce around the pile a thin layer (~5% MP diameter) of solid two-phase elements, to be assigned material parameters that represent changes (often degradation) in soil properties induced by pile installation – which is not explicitly simulated in the considered *wished-in-place* approach. Better representation of sliding and detachment along the soil-pile interface, as well as of water flow through discontinuities, may be achieved by using widthless interface elements of the kind

proposed by Cerfontaine et al. (2015). A drawback often associated with widthless interface elements is their relatively simplistic formulation from a constitutive standpoint, usualy based on perfect elasto-plasticity and hardly suitable to capture the complex cyclic behaviour of soil-steel interfaces – an interesting remedy to this issue has been recently proposed by Stutz et al. (2017).

Time integration algorithm. Standard algorithms for time integration in solid dynamics are suitable, such as the well-known Nermark's or HHT methods (Hughes, 1987). Algorithmic energy dissipation in time marching is usually beneficial in non-linear computations to damp spurious (non-physical) high-frequencies modes out of the calculated response (Kontoe et al., 2008). It should also be noted that, while implicit time integration combined with Newton-type iterations helps fulfilling global equilibrium, the selection of appropriate time-step size is most often driven by accuracy and stability of stress-strain integration at Gauss points – this aspect stands out most severily when sophisticated non-linear soil models are adopted (Watanabe et al., 2017).

3.2 Modelling of cyclic soil behaviour

The analysis of soil-MP interaction under ECL can only be as accurate as the constitutive modelling of cyclic soil behaviour, obviously a very relevant ingredient in integrated OWT models. Great efforts have been devoted in the past four decades to conceiving plasticity theories for cyclically loaded soils, e.g. in the frameworks of multi-surface plasticity (Mroz, 1967), bounding surface plasticity (Dafalias & Popov, 1975), generalised plasticity (Zienkiewicz & Mroz, 1984), hypoplasticity (Mašín, 2018) and hyperplasticity (Houlsby & Puzrin, 2007). Readers interested in these developments may refer to Prévost and Popescu (1996), Zienkiewicz et al. (1999) and di Prisco and Wood (2012).

The research overviewed in this paper focuses on OWTs in medium-dense/dense sandy soils, a case relevant to offshore wind developments in the North Sea. Special care has been taken about adopting state-of-the-art soil modelling, as shown in Corciulo et al. (2017a,b) and Kementzetzidis et al. (2018, 2019a). Despite fundamental differences in their formulations (Prévost, 1982), both multi-surface and bounding surface models can capture several aspects of cyclic sand behaviour, including stiffness degradation, hysteresis and deviatoric-volumetric coupling (leading to pore pressure build-up when drainage is hindered). However, after testing the performance of the UCSD multi-surface model (Elgamal et al., 2003; Yang et al., 2008), conceptual motivations have later led to embrace the family of SANISAND bounding surface models developed by Dafalias and co-workers. Since the launch of the first SANISAND model (Manzari & Dafalias, 1997), intensive work has been spent to overcome certain limitations of the original formulation, regarding fabric effects, hysteretic small-strain behaviour, response to radial stress paths, influence of principal stress axes rotation (Papadimitriou et al., 2001; Dafalias & Manzari, 2004; Taiebat & Dafalias, 2008; Petalas et al., 2019).

To date, the SANISAND version by Dafalias & Manzari (2004) – SANISAND04 – is still the most widespread with the following features:

- bounding surface formulation with kinematic hardening and Lode-angle dependence;
- adoption of the 'state parameter' concept (Been & Jefferies, 1985; Muir Wood et al., 1994). The model can capture the effects of varying effective confinement and void ratio, and thus simulate the response of loose to dense sands with a single set of parameters;
- contraction-to-dilation transition when the stress path crosses the *phase transformation surface*;
- *fabric tensor* to phenomenologically represent fabric effects triggered by load reversals following stages of dilative deformation.

As discussed in Section 4, the above model features impact altogether the numerical solution

of initial-boundary value problems. However, the conceptual advances fostered by SANISAND developments are not yet conclusive. Current research on offshore foundations (and not only) is continually stimulating the enhancement of cyclic modelling approaches – for example regarding SLS requirements threatened by the accumulation of soil deformations under long-lasting (high-cyclic) ECL. This matter is further addressed in Section 5.

From the standpoint of numerical integration, explicit stress-point algorithms are usually preferred over implicit methods for applications involving cyclic/dynamic loading and, therefore, frequent stress increment reversals. While the Forward Euler algorithm is the simplest in this area, adaptive Runge-Kutta methods with automatic error control should be adopted to combine accuracy and efficiency (Sloan, 1987; Tamagnini et al., 2000).

4 FROM NON-LINEAR SOIL–MP INTERACTION TO OWT DYNAMICS

The modelling concepts introduced in the previous section have been applied to the dynamic analysis of a real 8 MW OWT under different loading and geotechnical scenarios. The main structural details of the OWT – courtesy of Siemens Gamesa Renewable Energy – are provided in Fig. 7; the original design of the foundation – a monopile of 8 m diameter, 27 m embedded length and 62 mm wall thickness – was conceived for installation in North Sea dense sand. Due to the lack of thorough laboratory test data, a homogeneous deposit of Toyoura sand has been assumed, characterised by SANISAND04 model parameters provided by Dafalias & Manzari (2004). This deviation from reality, however, is not believed to prevent realistic conclusions regarding cyclic soil-MP interaction in water-saturated sand.

The following subsections address different aspects of OWT-MP-soil dynamics as emerging from 3D FE simulations of the 8 MW structure shown in Fig. 7. All results have been obtained through the open-source FE platform OpenSees[1] (McKenna, 1997; Mazzoni et al., 2007) – more details about OWT model set-up are available in Kementzetzidis et al. (2019a). Beyond its proven suitability for dynamic soil-structure modelling, OpenSees includes accessible implementations of stabilised *H1P1ssp* brick elements (McGann et al., 2015) and SANISAND04 (Ghofrani & Arduino, 2018).

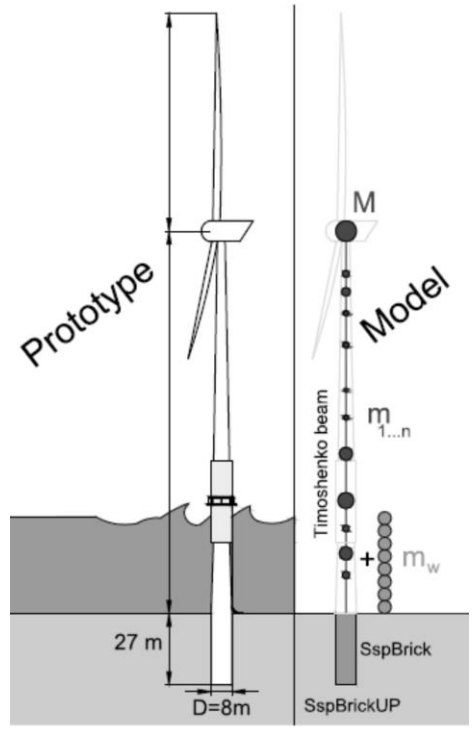

Fig. 7. Structural idealisation of the considered 8 MW OWT (modified after Kementzetzidis et al., 2019a).

4.1 OWT natural frequency shifts due to storm loading and seabed scour

After setting up the 3D FE model of the OWT-MP-sand system in Fig. 7, the dynamic response of the structure has been numerically analysed in

[1] http://opensees.berkeley.edu

relation to severe environmental loading. In particular, the 10 minutes time histories of wind/wave thrust forces in Fig. 8 have been considered[2] as representation of a 50-years return period storm (average wind speed of 47 m/s), including a 10 m-tall rogue wave hitting the structure after about 70 s. Under such loading conditions it is appropriate to assume the OWT to be in idling state, so that wind loading is mostly due to viscous drag along the structure. As mentioned in Section 2, an important design driver for OWTs is the tuning of the first bending eigenfrequency f_0 of the OWT over its compliant foundation (MP + soil). Advanced 3D modelling can be fruifully employed to foresee deviations of the structural performance from the desired *soft-stiff* range, for instance during exceptional storm events. For this purpose, it is beneficial to inspect the OWT response by means of time-frequency transformation. A suitable option is provided by the so-called S(Stockwell)-transform (Stockwell et al., 1996), e.g. applied by Kramer et al. (1996) to study the cyclic liquefaction of sandy sites.

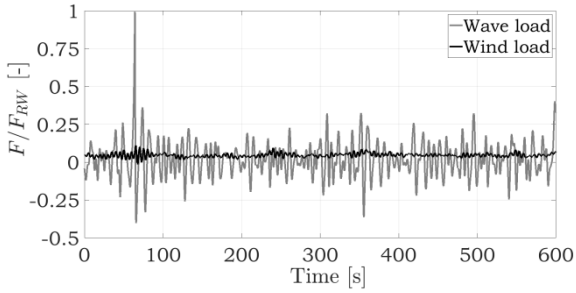

Fig. 8. Wind/wave thrust forces associated with a 50-years return period storm – average wind speed equal to 47 m/s (modified after Kementzetzidis et al., 2019a)

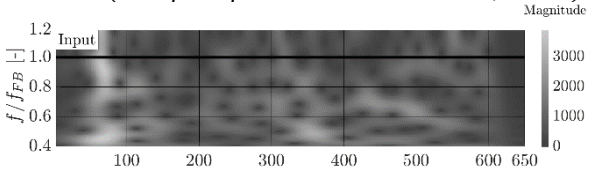

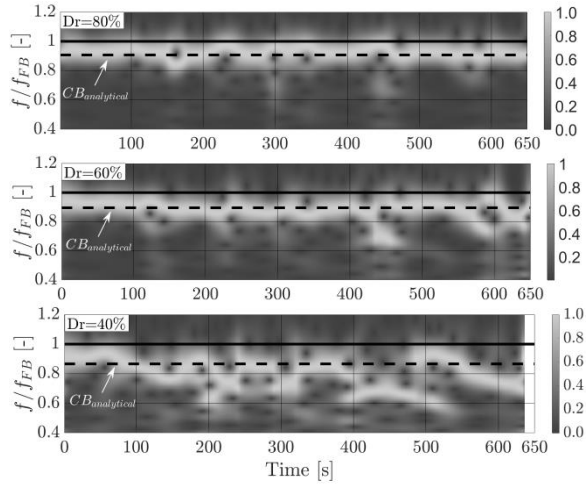

Fig. 9. S-plots of (top) input load (Fig. 8) and (up to bottom) hub displacement for Dr= 80%, 60%, 40%. Fixed-base natural frequency f_0/f_{FB} = 1. Colourbars indicate the amplitude of harmonics in the range (0.4–1.2)×f_0/f_{FB}. (modified after Kementzetzidis et al., 2019a)

S-transformation can show how the frequency content (and associated energy levels) of a signal evolves in time, which is here instrumental to tracking f_0 for an OWT subjected to severe ECL.

Fig. 9 reports S-plots of the total horizontal load applied to the OWT (top), and of the OWT hub displacement histories emerging from three different initial conditions – sand relative density (D_r) equal to 80, 60, 40%. Although unrealistic, the case D_r = 40% is purposely considered to mobilise high soil non-linearity, and thus warn about the detriments of poor geotechnical design. S-amplitudes in Fig. 9 relate the colourbars on the side, and normalised at each step with respect to the maximum value across the frequency axis – this allows to emphasise the peak frequency[3] with the same light-grey colour along the 10 minutes history. Plotted for the three cases are are also analytical estimates of f_0 on compliant base ($CB_{analytical}$) as per Arany et al. (2017) – dashed lines, see calculation details in Kementzetzidis et al. (2019a). S-plots reveal strong dependence of

[2] Force amplitudes in Fig. 8 are normalised with respect to the rogue wave amplitude (F_{RW}).

[3] Frequencies in Fig. 9 are normalised with respect to the natural frequency of the OWT on a fixed base (f_{FB}).

the OWT response on the initial relative density, as well as on the amplitude and frequency content of the input loading. When the OWT is founded on stiff sand (D_r = 80%), its response in the frequency domain exhibits a single main peak at the first eigenfrequency, with only modest transient shifts; similar conclusions are mostly applicable to the D_r = 60% case as well. In other words, f_0-shifts should not be a concern when the monopile is designed according to current practice. In this case, even analytical predictions (Arany et al., 2017) return robust lower-bound estimates of the f_0 values resulting from 3D FE simulations.

The OWT response becomes quite different for D_r = 40%. Fig. 9 (bottom) shows in this case a very irregular evolution of the peak frequency. Such a response marks a transition from "resonance-dominated" to "input-dominated" regime – note that the most evident drops in peak frequency at the hub occur at frequencies associated with high energy content in the input S-transform. This kind of structural performance is clearly undesired, and may be regarded here as the outcome of poor geotechnical design.

The global picture emerging from Fig. 9 can be further understood through its relation to the hydro-mechanical response of the soil around the MP. With reference to the check-point B_R in Fig. 10a, Fig. 10b illustrates the time evolution of the local pore pressure u at varying initial D_r (u is normalised with respect to the current total mean pressure p). It is interesting to note that the inception of "chaotic" time-frequency response for D_r = 40% correlates very well with the time (t = 300 s) at which the pore pressure ratio u/p goes beyond 0.9 – at point B_R and, it could be

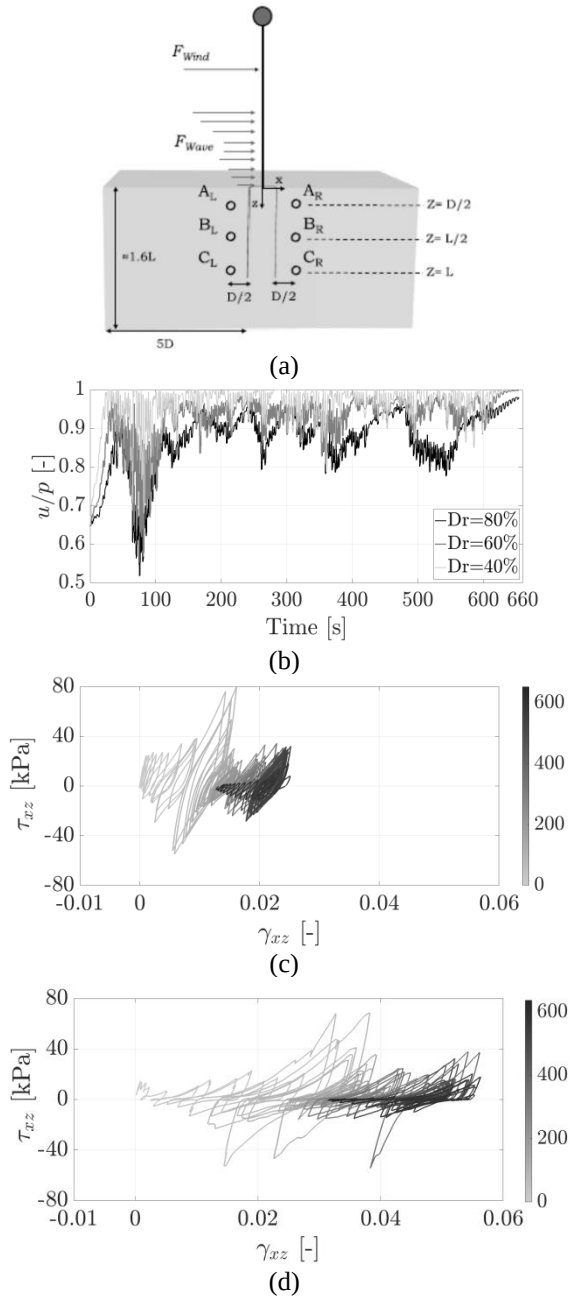

Fig. 10. (a) 8MW OWT model and location of control points; (b) pore pressure evolutions at point B_R; shear stress-strain plots at B_R for (c) Dr = 80% and (d) D_r = 40% (modified after Kementzetzidis et al., 2019a)

verified, at all other control points in Fig. 10a (see Kementzetzidis et al., 2019a). From that time

onward the soil around the pile can only mobilise very low stiffness due to the reduced effective confinement, with an obvious effect on the global compliance of the foundation. The stress-strain response predicted by SANISAND04 is in turn consistent with pore pressure build-up: although significant non-linearity and dissipative behaviour are already evident in Fig. 10c for D_r = 80%, the D_r = 40% case displays the same features more extremely, with severe loss in stiffness/strength and accumulation of irreversible shear strains. Partial liquefaction (Fig. 10b), however, does not extend to the whole soil deposit: the resistance available at farther soil locations is not fully compromised, with positive impact on the OWT performance.

The mentioned transition from resonance- to input-dominated OWT response (Fig. 9) is also affected by the amount of energy dissipated at the foundation. Large values of foundation damping promotes quick dissipation of transient "eigen-motion" components of the structure, letting external loading dominate structural vibrations. The numerical rotor-stop tests documented in Kementzetzidis et al. (2019a) confirm the high damping generated at the foundation during the 50-years storm in Fig. 8. It is also worth recalling that accurate analysis of dissipative phenomena is highly relevant to FLS checks (Section 2), as they affect the amplitude of the stress levels experienced by the steel during the OWT life.

The numerical results discussed so far support the conjecture of Kallehave et al. (2012): pore pressure effects may negatively impact the OWT dynamic performance, especially in presence of under-designed foundations. However, current design practice would hardly result in a structural response as poor as in the D_r = 40% case (Fig. 9), unless "unexpected" circumstances arise during operations. A possible event of this kind may be the erosion of

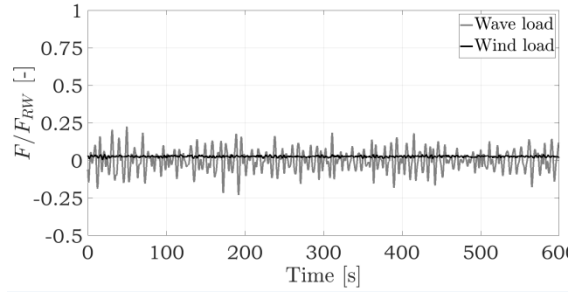

Fig. 11. Wind/wave thrust forces associated with a storm without rogue wave – average wind speed equal to 24 m/s (modified after Kementzetzidis et al., 2019a)

soil around the monopile, also termed *seabed scour*. Scour takes place when near-bed shear stresses are such that soil sediments can be displaced from the original location (Prendergast et al., 2015). DNV-GL design guidelines recommend to perform ULS and SLS checks accounting for likely scour scenarios (scour depth up to 1.3 MP diameters), perhaps caused by ineffective scour protection.

To study the impact of scour on f_0, the same OWT in Fig. 7 has been numerically analysed in combination with the wind/wave loading history in Fig. 11, associated with an average wind speed of 24 m/s – for better comparison, forces are again normalised with respect to the amplitude of the rogue wave in Fig. 8. For simplicity, three scenarios of uniform scour have been considered –removal in the FE model a superficial layer of sand (D_r = 80%) of thickness H_{scour} = 0 (no scour), 0.5, 1.25 MP diameters.

In Fig. 12a S-plots are used again to visualise in the time-frequency domain the response at the OWT hub at varying scour depth. Looking at the S-transform of the load input (Fig. 12a-top), it is apparent that increasing H_{scour} has a twofold effect: (i) it causes a reduction of the average ratio between f_0 and the reference fixed-base value f_{FB}; (ii) as H_{scour}/D approaches 1.25, the previous transition towards input-dominated vibrations is observed. These two effects are interrelated sides of the same coin. As soil confinement around the monopile reduces due to

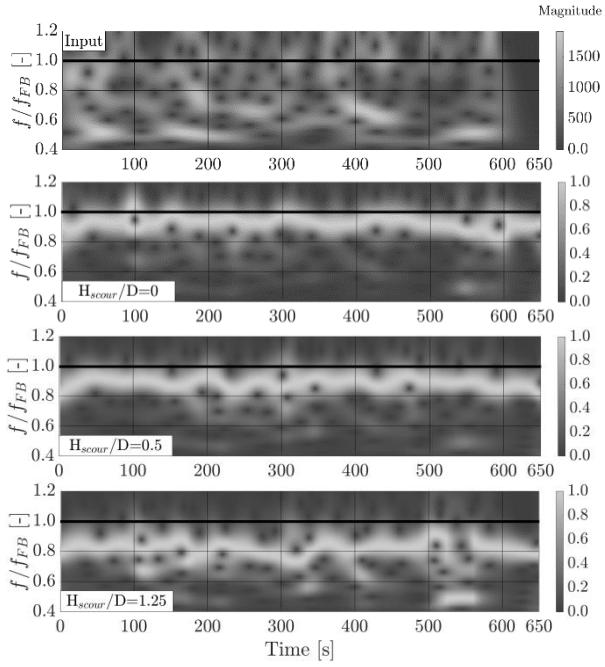

(a)

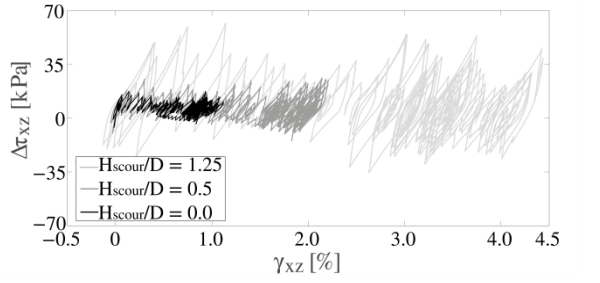

(b)

Fig. 12. (a) S-plots of (top) input load (Fig. 11) and (up to bottom) hub displacement for H_{scour}/D = 0, 0.5, 1.25 (Dr = 80%); (b) shear stress-strain plots for a soil location next to the MP tip at varying H_{scour}/D

erosion, the remaining soil is strained more severely under the storm in Fig. 11. The hydro-mechanical response of the soil reaches levels of non-linearity that keep the structure from functioning in the intended *soft-stiff* range. This fact is elucidated by Fig. 12b, reporting the local shear stress-strain response in the soil close to the MP tip: increasing dissipation and strain accumulation occur at higher H_{scour}. The results in Fig. 12 appear in line with recent experimental evidence (Li et al., 2018), and raise design concernes that may not be properly addressed through simplistic models.

4.2 Effects of long-term re-consolidation

In Section 4.1 transient shifts in f_0 have been numerically investigated as a result of short storm events (duration equal to 10 mins), inducing pore-pressure build-up and related cyclic softening of the soil. As a further step, it is relevant to explore whether losses in soil confinement will be permanent or not after the storm. For this purpose, the numerical case presented in Kementzetzidis et al. (2018) is summarised herein. The same reference 8 MW OWT is subjected to the more complex load history in Fig. 13, comprising multiple loading sub-events and after-storm reconsolidation, during which excess pore pressure dissipation can take place. In this spirit, the load history (sum of wind and wave loads) illustrated in Fig. 13 is considered – total duration of more than 2 hours:

1. 150 s of weak loading, mobilising relatively small strains in the soil around the pile;
2. 1200 s of strong storm loading (average wind speed of 24 m/s), inducing transient f_0-drops;
3. 150 s of the previous weak loading to explore after-storm effects on f_0;
4. 1.7 hours (6000 s) of no loading to allow for excess pore pressure dissipation;
5. 150 s of weak loading to detect regains in f_0 enabled by soil re-consolidation. As previous excess pore pressures are mostly dissipated at the beginning of this stage, any differences with respect to pre-storm OWT response can only be due to permanent effects of plastic straining and void ratio changes.

To reduce the burden of a long (sequential) 3D FE simulation, the mesh in Fig. 14, coarser than the instance in Fig. 5b, has been adopted – the soil control points A, B, C are also highlighted in the same figure. The evolution of the frequency content in the OWT response has been monitored through the S-transform of the

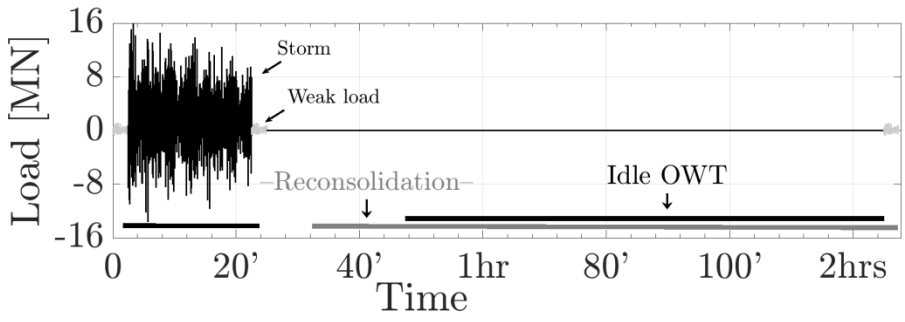

Fig. 13. Assumed load time history – sum of wind and wave thrusts (modified after Kementzetzidis et al., 2018)

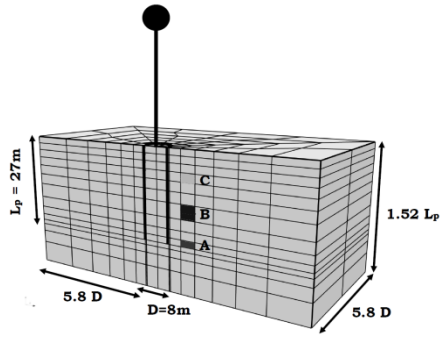

Fig. 14. 3D coarser soil mesh (~950 H1P1ssp bricks) adopted for ~2hrs FE simulation – A, B, C are control points considered for post-processing (modified after Kementzetzidis et al., 2018)

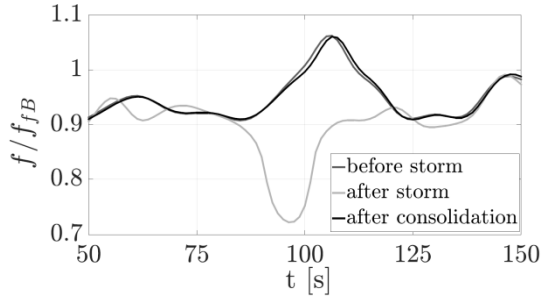

Fig. 16. Time evolution of the OWT peak frequency during the three weak loading stages in the compound load history in Fig. 13 (modified after Kementzetzidis et al., 2018)

horizontal displacement at the hub. Since the S-

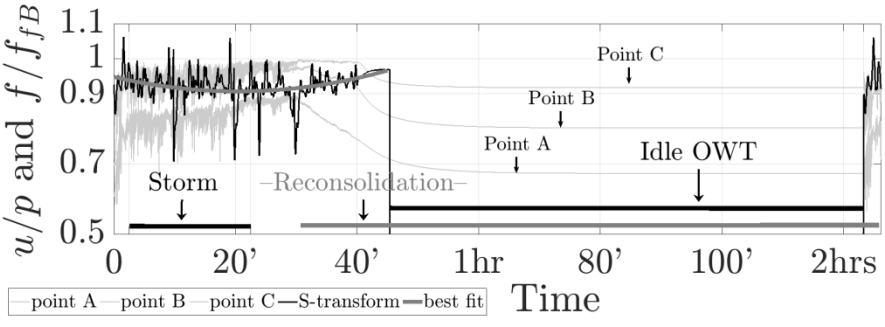

Fig. 15. Thick black line: normalised OWT peak frequency, along with best quadratic fit; dotted lines: u/p ratios at the control points in Fig. 14 (modified after Kementzetzidis et al., 2018)

transform returns (time-varying) frequency content within a relevant band, the outcrop values

related to the maximum (normalised) S-amplitude at each time-step can be used to track f_0-drops with respect to the fixed-base value f_{FB}.It is evident in Fig. 15 that the OWT experiences transient natural frequency shifts during the storm – as also underlined by the quadratic time-fit of the peak frequency extracted from the S-transform. At the same time, an increase in pore pressure ratio u/p is observed at the three control points indicated in Fig. 14. The local minimum of the fitting parabola lies close to the time of load removal, which hints that f_0 recovery starts at the end of a storm. When free structural vibrations are entirely damped out after the storm, soil re-consolidation starts to dominate the response (Fig. 15). It is noted that f_0 tends to recover its pre-storm value as re-consolidation proceeds. When excess pore pressures are dissipated up to the shallowest control point C, the natural frequency of the OWT appears to be completely restored. As a further confirmation, Fig. 16 shows that pre-storm and after-consolidation responses of the OWT are practically identical as to their S-representation. This leads to claim the existence of a sort of "self-healing" mechanism associated, in the considered analysis framework, to soil re-consolidation.

Obviously, the conclusions drawn after this application example are not only specific of geometrical and loading settings, but also of the adopted SANISAND04 model calibrated for Toyoura sand.

4.3 Towards MP-soil macro-modelling

The examples discussed so far give an impression of the possibilities of advanced geotechnical modelling in offshore wind research. At the same time, however, it should be acknowledged that its direct application to engineering practice is exactly straightforward, due to computational burdens, intrinsic model limitations, dearth of experimental data for parameter calibration, etc. These and other factors hinder daily use of 3D FE modelling in engineering design, normally based on more user-friendly *p-y* 1D methods.

It is also possible to formulate "0D" macro-models, in which soil-foundation interaction is lumped into a small number – 6 at most for 3D problems – of constitutive relationships between the forces and displacements describing the statics/kinematics of the considered foundation. This approach – also known as *macroelement modelling* – was first devised for the integrated modelling of mobile jack-up platforms (Schotman, 1989), then applied to a variety of shallow foundation problems (Nova & Montrasio, 1991; Pisanò et al., 2014, Houlsby, 2016), also including dynamic/seismic loading conditions (di Prisco and Pisanò, 2011). More recently, advanced macroelements have been proposed to capture the complex behaviour of piled foundations (Li et al., 2016), with some instances of application to OWT monopiles (Houlsby et al., 2017; Page et al., 2019a,b). Regardless of the specific foundation type, macroelement models need accurate description of soil-structure interaction, including – in cyclic loading problems – stiffness degradation and energy dissipation effects. In presence of higher loading frequencies, such macro-interaction will be also "dynamic", i.e. frequency-dependent.

All the mentioned ingredients are not only challenging to lumpt into a simple 0D (plasticity) formulation, but also to investigate through experimental or numerical studies. Integrated 3D FE models can positively inspire such developments, as shown by Corciulo et al. (2017b) in relation to MP-supported OWTs – Fig. 17a illustrates a simplified OWT model, with soil-monopile interaction condensed into two (uncoupled) springs. With reference to the results discussed in Section 4.1 for the input storm in Fig. 8, it is shown in Figs. 17b-c how the moment-rotation response at the MP head evolves in time, with average stiffness (dashed lines) decreasing as more severe plastic straining

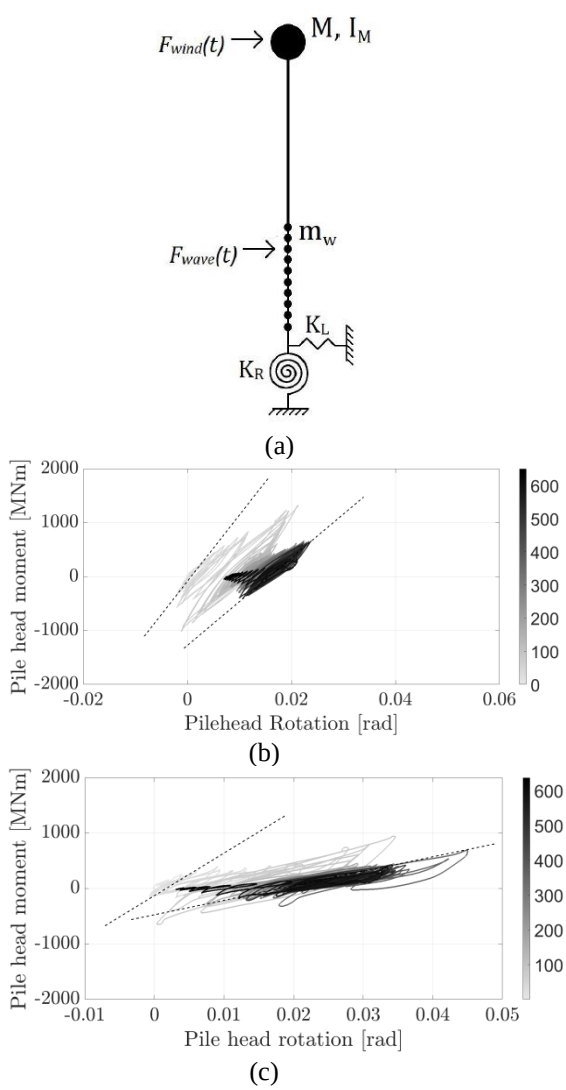

Fig. 17. (a) simplified structural model of a MP-supported OWT (modified after Corciulo et al., 2017b); time-evolution of the rotational MP head stiffness for the storm input in Fig. 8 with Dr equal (b) 80% and (c) 40% (modified after Kementzetzidis et al., 2019a)

takes place in the soil around the foundation. In particular, rotational stiffness degradation[4] from 99 to 79 GNmrad^{-1} and from 60 to 34 GNmrad^{-1} are observed in the cases D_r = 80% (Fig. 17b) and D_r = 40% (Fig. 17c), respectively – see details in Kementzetzidis et al. (2019a). This kind of input to macroelement modelling seems particularly valuable, as it already includes non-linear hydro-mechanical effects hard to account for otherwise. It seems prudent to say that, when the soil is strained beyond the *volumetric shear threshold* (i.e. beyond the onset of deviatoric-volumetric deformation coupling), macro-models that neglect pore pressure effects cannot reproduce aspects of MP-soil interaction clearly emerging from advanced 3D FE modelling.

3D FE simulations and derived macro-models can also aid the analysis of OWTs under seismic loading (Kaynia, 2018; Vacareanu et al., 2019), although with additional complexity arising from dynamic amplification and, in sandy soils, cyclic liquefaction. Even when disregarding soil instabilities, the problem of properly representing frequency-dependence in MP-soil dynamic interaction is still open. Work on this specific subject is presently ongoing at TU Delft (Versteijlen et al., 2017; Kementzetzidis et al., 2019b), although not covered here for brevity.

5 HIGH-CYCLIC SAND MODELLING FOR SLS CHECKS IN MP DESIGN

The serviceability of monopiles is also related to preventing their excessive deformation under long-lasting environmental loading – see check 4 in Section 2 (Kuo et al., 2011). The problem of predicting cyclic deformations of laterally loaded piles is not new in geotechnical engineering, but is presently receiving renewed attention with reference to offshore wind developments. In recent years, a number of experimental studies have been devoted to studying the cyclic lateral tilting of stiff piles (Leblanc et al, 2010; Rudolph et al., 2014; Li et al., 2015; Nicolai et al, 2017; Truong et al., 2018, Abadie et al., 2018). Still with reference to monopiles in sandy soils, tilt accumulation laws have been empirically derived

[4] In this illustrative example it was not attempted to distinguish rotational-translation stiffness couplings.

from small-scale tests. New insight into the evolution of soil stiffness and post-cyclic MP capacity has emerged, sometimes contraddicting "traditional beliefs" regarding presumed "degradation" phenomena in cyclically loaded foundations (API, 2014; DNV-GL, 2016).

In parallel with experimental activities, several researchers are also exploring methods for numerically predicting cyclic MP tilt. One of the main challenges in this area is the high number of loading cycles experienced by OWTs during their operational life – up to $10^{7\text{-}8}$ (Leblanc et al., 2010). As a consequence, MP tilt predictions are non-trivial to obtain for at least two reasons: (a) time-domain, step-by-step analysis (*implicit*, in the terminology of Niemunis et al., 2005) is computationally very demanding; (b) even if implicit computations were viable, the literature still lacks fully reliable models reproducing soil behaviour under so-called *high-cyclic* loading. Alternatively, *explicit* methods have also been considered, in which permanent soil straining is directly linked to the number of loading cycles *N*. In this framework, the relationship between accumulated strains and N is given by empirical laws derived from high-cyclic laboratory test results. Valuable examples of explicit methods adopted in the 3D FE analysis of tilting monopiles are provided e.g. by Achmus et al. (2009), Jostad et al. (2014), Wichtmann et al. (2017), Chong & Pasten (2018).

Regarding implicit approaches based on cycle-by-cycle analysis, the experimental evidence provided by the aforementioned studies is being mainly reproduced via special macro-models, as proposed e.g. by Houlsby et al. (2017). However, most recent studies are making a clear point about the need to link global MP-soil interaction to the local high-cyclic behaviour of the soil subjected to a variety of loading and boundary conditions (Cuéllar et al., 2009). Such a need is clearly noted, for instance, by Abadie et al., (2018):
"*It would be of great interest to analyse the soil behaviour down the pile and correlate the macro response observed in this paper to the local pile behaviour, and also to soil element behaviour.*"
or by Truong et al. (2018):
"*It is of interest to examine whether standard cyclic triaxial testing can be used to provide guidance to designers on the likely value of α in other sand types. […] Triaxial cyclic testing can provide insights for designers into expected lateral cyclic response in sands for which no previous experience exists.*".

These statements have been the premises to the TU Delft research on the (implicit) modelling of high-cyclic sand behaviour, and its ongoing application to the 3D FE analysis of pile tilt.

5.1 SANISAND-MS: a memory-enhanced model capturing cyclic sand ratcheting

The SANISAND04 model described in Section 3.2 (Dafalias & Manzari, 2004) allows to look deep into MP-sand interaction, including the interplay of dynamics, sand porosity and pore pressure effects. Owing to this conceptual tool, the performance of OWTs in presence of exceptional external conditions (severe storms, seabed scour, etc.) can be analysed and grasped in a way not allowed by simplified engineering methods. However, despite its notable merits, SANISAND04 is clearly quite far from perfection, with some of its drawbacks being most incovenient for offshore wind foundation problems. Among them, it is important to reliably predict high-cyclic strain accumulation (*soil ratcheting*), as well as the timing and extent of pressure build-up when water drainage is hindered. Regarding the former issue, none of the abovementioned SANISAND models can quantitatively reproduce the high-cyclic (drained) ratcheting of sands (Houlsby & Puzrin, 2007), nor its dependence on input loading parameters. To mitigate this limitation Liu et al. (2018a) recently proposed a new SANISAND model with ratcheting control. Liu et al.'s model is built upon the parent SANISAND04 model, and enhanced according to the notion of *memory surface* (Corti et al., 2016) – hence the name SANISAND-MS. The memory locus is introduced to phenomenologically track fabric

effects at the micro-scale, and thus improve the simulation of cyclic sand behaviour.

Compared to Dafalias & Manzari's model, SANISAND-MS adopts a third circular locus in the normalised deviatoric stress ratio plane, the memory surface (Fig. 18), which evolves during soil straining so as to (i) modify its size/position in reflection of fabric changes, (ii) always enclose the yield surface, (iii) influence changes in sand stiffness and dilatancy. Other ingredients of SANISAND04 are mostly unchanged. Continual efforts are being devoted to validating the model against laboratory test data from the literature, trying to address as many loading conditions as possible – including cyclic triaxial, simple shear and oedometer tests (Liu at al., 2018a).

The performance of SANISAND-MS in drained cyclic triaxial tests on anisotropically consolidated specimens (Fig. 19a) is compared to SANISAND04's in Fig. 19b-c. It is self-apparent that SANISAND-MS can prevent the irrealistic overestimation of sand ratching yielded by the parent model, and thus capture cyclic strain accumulation as observed in laboratory tests.

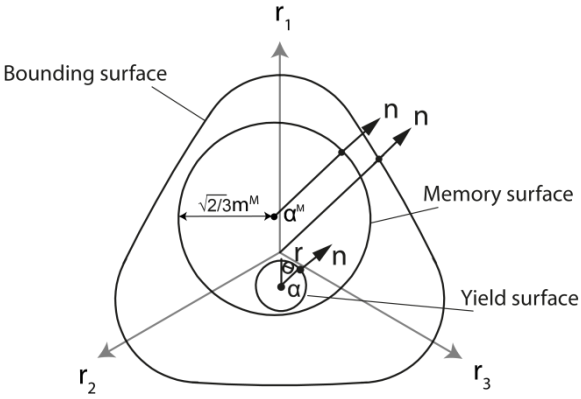

Fig. 18. Relevant model loci, stress ratios and directions in SANISAND-MS (modified after Liu & Pisanò, 2019)

Fig. 20 supports the quantitative accuracy of the new model in light of comparisons to measured strain accumulation trends at varying governing factors (Wichtmann, 2005), namely initial mean pressure (Fig. 19a), initial void ratio (Fig. 19b) and cyclic stress deviator amplitude (Fig. 19c).

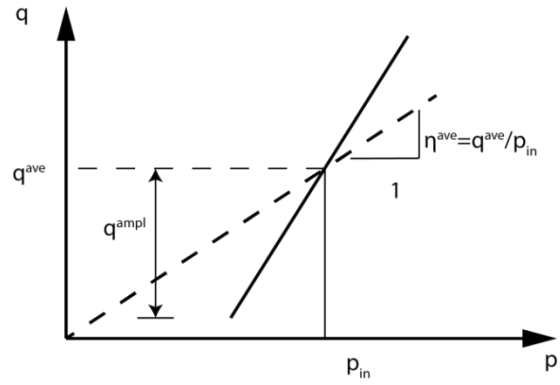

(a)

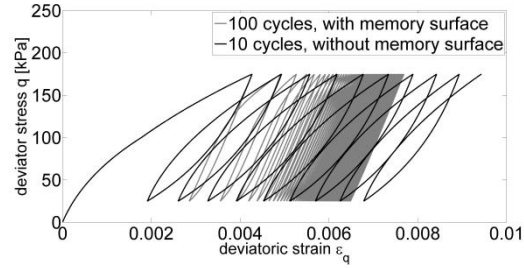

(b)

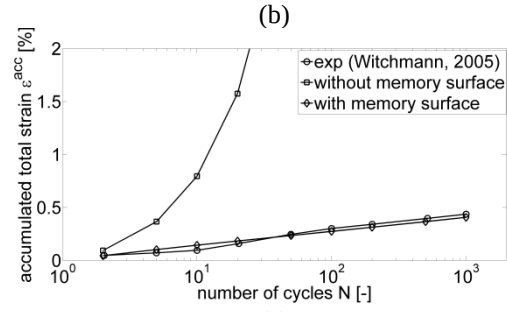

(c)

Fig. 19. (a) Stress path in cyclic triaxial tests on anisotropically consolidated specimens; (b) influence of the memory surface formulation on the response to asymmetric drained triaxial loading, and (c) comparison to laboratory test results in terms of accumulated total strain (experimental data from Wichtmann, 2005).

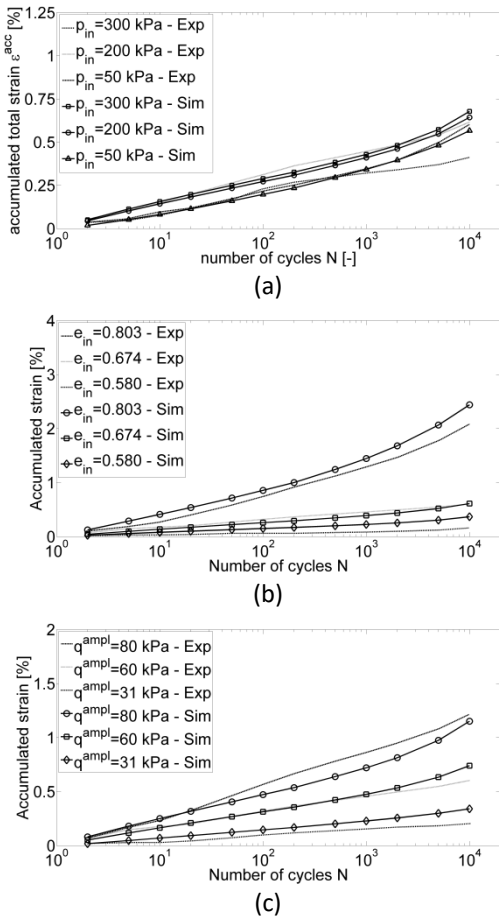

Fig. 20. Comparison between SANISAND-MS and laboratory test results about the influence of (a) initial mean pressure, (b) initial void ratio, and (c) cyclic deviatoric stress amplitude – same stress path as in Fig. 19a (test data from Wichtmann, 2005).

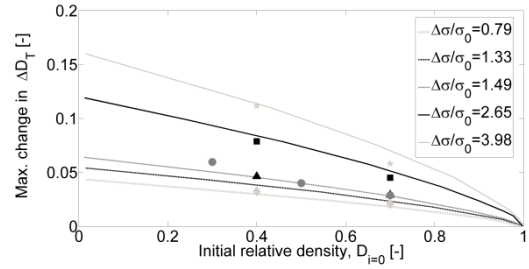

Fig. 21. Maximum changes in relative density (ΔD_T) against initial/pre-cyclic values $D_{i=0}$ – dash lines: interpolation of Park & Santamarina's data; markers: SANISAND-MS simulations (modified after Liu and Pisanò, 2019)

More recently, the suitability of SANISAND-MS has also been investigated with respect to cyclic oedometer tests on dry sand, particularly about the ability to predict so-called *terminal densities* – which refers to sands eventually approaching under cyclic loading an asymptotic void ratio, depending on mechanical properties, loading programme and boundary conditions.
In Liu & Pisanò (2019a) the cyclic oedometer tests results from Park & Santamarina (2018) are successfully reproduced through SANISAND-MS for Ottawa sand specimens subjected to different combinations of initial void ratio and cyclic axial stress amplitude (Fig. 21).

The suitability of the memory surface approach is not limited to drained ratcheting behaviour, but seems also extremely promising in relation to undrained response and cyclic pore pressure build-up. Research on this aspect is currently ongoing at TU Delft (Liu et al., 2018b; Liu et al., 2019b).

5.2 3D FE analysis of cyclic monopile tilt

The SANISAND-MS model described above is suitable to reproduce (drained) sand ratcheting over thousands of loading cycles and diverse stress paths (Liu et al., 2018a; Liu & Pisanò, 2019a). This confidence about the performance of the model suggests to attempt its use in the 3D FE analysis of MP tilt. As previously noted, the adoption of 3D modelling for long-lasting cyclic loading histories may not (yet) be viable in daily engineering practice, due to computational costs. Nevertheless, advanced modelling approaches can certainly add to the understanding of complex soil-structure interaction mechanisms, and inspire the conception of engineering methods.

In the examined case, it should be recognised that the tilting response of MPs is most likely affected by the complexity of environmental loading, featuring variable amplitude, spatial orientation and frequency spectrum. Such features should be expected to induce in the soil loading conditions not commonly investigated in

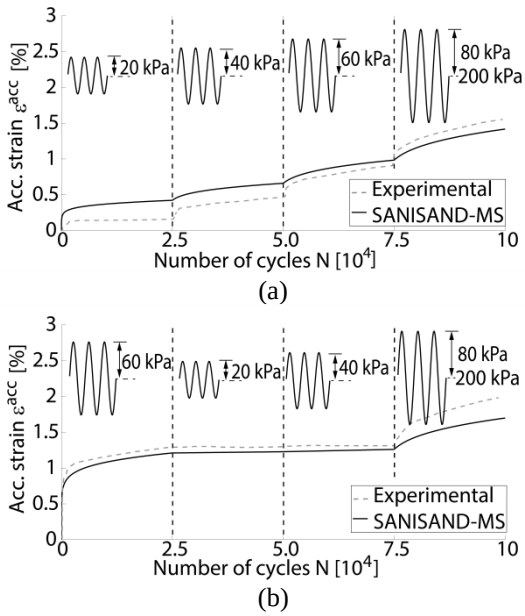

Fig. 22. Relationship between cyclic strain accumulation and sequence of cyclic load packages in biased one-way triaxial tests. Comparison between experimental results (data from Wichtmann, 2005) and SANISAND-MS simulations (Liu, 2020)

laboratory tests, and hardly considered in the validation of constitutive models. An exception in this area is the experimental work carried out in Germany by Wichtmann and co-workers (Wichtmann, 2005; Wichtmann et al., 2010; Wichtmann & Triantafyllidis, 2017), who studied how the specific sequence of different cyclic load packages can influence the ratching behaviour. The resulting experimental evidence supports at the material level the well-known *Miner's rule*, originally devised in relation to metal fatigue (Miner, 1945). Accordingly, the specific sequence of cyclic load packages only slightly affects final strain accumulation, also in sand specimens. Fig. 22 provides an instance of this observation, regarding two medium-dense sand specimens subjected to 10^5 biased one-way triaxial cycles (as in Fig. 19a) of either increasing (Fig. 22a) or alternating (Fig. 22b) deviatoric stress amplitude. The same figure also shows SANISAND-MS simulations obtained with material parameters calibrated for the Karlsruhe sand tested in the laboratory (Liu et al., 2018a). Owing to the memory surface mechanism, SANISAND-MS can reproduce the Miner-like response observed in the experiments (Liu, 2020). Particularly, the transition from higher to lower cyclic load amplitude seems to inhibit strain accumulation, an occurrence captured by the model through the higher cyclic stiffness associated with stress state within the memory surface. Significant ratcheting is predicted upon expansion of the memory domain, which happens when the stress path hits new absolute maxima. These considerations have important engineering implications, e.g. about identifying the loading events that in reality will cause significant MP tilt – seemingly, only the most severe.

SANISAND-MS' performance is not only encouraging at the sand specimen level. Currently, the model is being tested in the 3D FE simulation of cyclic MP tilt (Liu, 2020). Preliminary results are presented herein for the problem illustrated in Fig. 23, regarding a monopile (diameter D = 4 m) in Karlsruhe dry sand (initial D_r = 57%) subjected to cyclic lateral loading applied at the soil surface level. After space discretisation and soil gravity loading, quasi-static horizontal cyclic loading has been applied according to two loading programmes: (1) monotonic lateral loading up to 0.8 MN, followed by two cyclic load packages (100 cycles each) of 0.4 MN and 1.2 MN amplitude; (2) same monotonic loading, followed by a cyclic load sequence with reversed amplitudes.

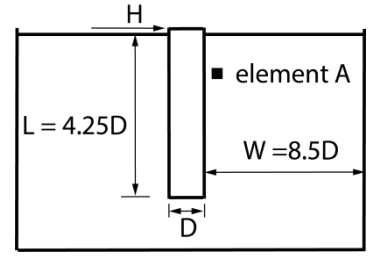

Fig. 23. Case example selected for the 3D FE simulation of cyclic MP tilt based on SANISAND-MS

Lateral displacement trends at the MP head are plotted in Fig. 24 for both cyclic load sequences. Displacement accumulation plots are aligned with the multi-amplitude ratcheting behaviour exemplified for single sand specimens in Fig. 22. The MP tilting rate evolves with the number of cycles depending on the load package sequence, and decreases significantly as packages of decreasing cyclic amplitude are considered (Fig. 24b). 3D FE results support the idea that the final accumulated displacement is mostly determined by strongest packages, a fact also corroborated by the experimental results in Li et al. (2015), Troung et al. (2018), Abadie et al. (2018). It appears that the aforementioned Miner's rule upscales from the level of soil specimen to the global foundation level. The use of a cyclic soil model with ratcheting control, SANISAND-MS, is key to capturing such behaviour in 3D simulations, and can help unveil relevant relationships among external loading, evolution of soil state and resulting MP tilt (Liu, 2020).

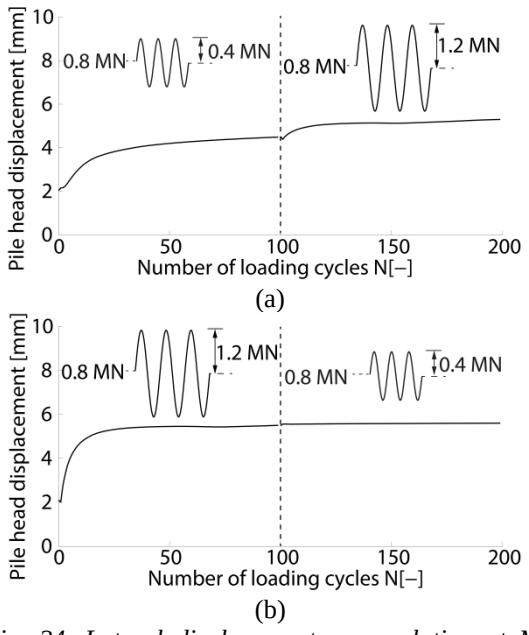

Fig. 24. Lateral displacement accumulation at MP head for cyclic load sequence (a) 1 and (b) 2 (Liu, 2020)

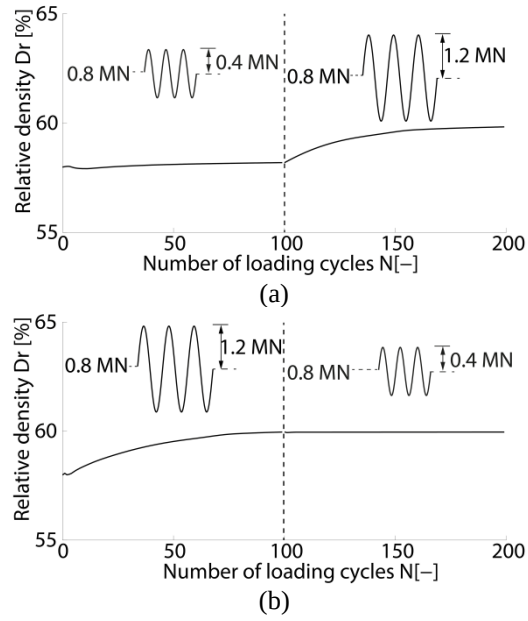

Fig. 25. Variation in relative density obtained at element A in Fig. 23 for cyclic load sequence (a) 1 and (b) 2 (Liu, 2020)

Local sand response is illustrated in terms of relative density evolution in Fig. 25 for the control element A in Fig. 23. Sand densification takes place around the pile in a Miner-like manner, confirming the occurrence of soil mechanisms described by Cuéllar et al. (2009).

Although preliminary, the results in Figs. 24-25 open to a whole thread of numerical modelling research, focused on the 3D analysis of sand ratcheting effects in laterally loaded monopiles. This line of work will contribute in the near future to quantifying the influence of different governing factors on monopile tilt.

6 CONCLUDING REMARKS

This paper presented an overview of recent research carried out at TU Delft on the numerical modelling of soil-structure interaction in offshore wind turbines, particularly for the common case of monopile foundations in sandy soils.

Modelling concepts and practical set-up issues were covered in relation to 3D FE models capable of integrating the response of wind turbine,

foundation and surrounding soil. The relevance of effective-stress-based analysis with advanced modelling of soil behaviour was stressed as a way to adequately reproduce dynamic consolidation processes in the seabed induced by structural vibrations. Despite significant complexity and computational burdens, 3D FE modelling was recognised as a powerful addition to traditional engineering methods, allowing for deeper design checks after preliminary foundation sizing.

The approaches discussed herein appear suitable to investigate possible shifts in OWT natural frequency caused by environmental loading and/or seabed scour; at the same time, modes and governing factors of energy dissipation around the foundation (damping) can be inspected and quantified. Beyond enabling more detailed analysis, the outcomes of 3D FE models can also support the conception and calibration of more efficient lumped models of soil-foundation interaction (macro-models), particularly useful for long-lasting time-domain calculations.

The problem of prolonged environmental loading was also linked to a specific monopile serviceability check, namely the accumulation of permanent lateral tilt. In order to complement experimental and macro-modelling studies, the problem of high-cyclic monopile tilt was addressed from a 3D FE modelling perspective. In this context, the memory-enhanced plasticity sand model developed at TU Delft, SANISAND-MS, was briefly described, and its performance demonstrated against experimental data from the literature. It was clarified that accumulating soil deformations during cyclic loading (ratcheting response) are major responsible for monopile tilt, in a way that 3D FE computations can help explore at a more detailed scale than allowed by macro-models. Ongoing work on improving and validating SANISAND-MS is foreseen to impact the understanding of monopile tilting in offshore environments.

The work summarised in this overview opens to numerous developments, such as extension to offshore wind structures interacting with different soil types (clays, silts, calcareous sands) and more realistic loading conditions. Further studies about seismic soil-foundation interaction issues are becoming increasingly relevant as new offshore wind farms are installed in seismically active regions. Further opportunities for high-fidelity integrated 3D FE modelling also lie in the explicit inclusion of sea-wave loading in fully coupled structure-fluid-soil analysis.

7 ACKNOWLEDGEMENTS

This paper is associated with the European Bright Spark Lecture delivered by the author at the XVII European Conference on Soil Mechanics and Geotechnical Engineering (ECSMGE-2019). Its contents summarise research carried out at TU Delft over the past four years by the author in cooperation with several colleagues. Special gratitude and acknowledgements go to E. Kementzetzidis, H.Y. Liu, and A.V. Metrikine (TU Delft), J. A. Abell (Universidad de los Andes), A. Diambra (University of Bristol)., S. Corciulo and O. Zanoli (Rina Consulting), W.G. Versteijlen and A. Nernheim (Siemens Gamesa Renewable Energy). The final review of this manuscript by G. Della Vecchia (Politecnico di Milano) is also warmly appreciated.

8 REFERENCES

Aasen, S., Page, A. M., Skau, K. S., & Nygaard, T. A. 2017. Effect of foundation modelling on the fatigue lifetime of a monopile-based offshore wind turbine. *Wind Energy Science*, 2(2), 361-376.

Abadie, C. N., Byrne, B. W., & Houlsby, G. T. 2018. Rigid pile response to cyclic lateral loading: laboratory tests. *Géotechnique*, 1-14, DOI: 10.1680/jgeot.16.P.325.

Achmus, M., Kuo, Y. S., & Abdel-Rahman, K. 2009. Behavior of monopile foundations under cyclic lateral load. *Computers and Geotechnics*, 36(5), 725-735.

API. 2014. Recommended Practice 2A-WSD. Planning, Designing, and Constructing Fixed

Offshore Platforms - Working Stress Design. American Petroleum Institute, 22 edition.

Arany, L., Bhattacharya, S., Macdonald, J. H., & Hogan, S. J. 2015. A critical review of serviceability limit state requirements for monopile foundations of offshore wind turbines. In Proc. Offshore Technology Conference. Houston (USA).

Arany, L., Bhattacharya, S., Macdonald, J., & Hogan, S. J. 2017. Design of monopiles for offshore wind turbines in 10 steps. *Soil Dynamics and Earthquake Engineering*, 92, 168-152.

Barari, A., Bagheri, M., Rouainia, M., & Ibsen, L. B. 2017. Deformation mechanisms for offshore monopile foundations accounting for cyclic mobility effects. *Soil Dynamics and Earthquake Engineering*, 97, 439-453.

Been, K., & Jefferies, M. 1985. A state parameter for sands. *Géotechnique*, 35(2), 99–112.

Biot, M. A. 1956a. Theory of propagation of elastic waves in a fluid-saturated porous solid. II. Low frequency range. *The Journal of the Acoustical Society of America*, 28(2), 168-178.

Biot, M. A. 1956b. Theory of propagation of elastic waves in a fluid-saturated porous solid. II. Higher frequency range. *The Journal of the Acoustical Society of America*, 28(2), 179-191.

Balog, I., Ruti, P. M., Tobin, I., Armenio, V., & Vautard, R. 2016. A numerical approach for planning offshore wind farms from regional to local scales over the Mediterranean. *Renewable energy*, 85, 395-405.

Bhattacharya, S. 2019. *Design of foundations for offshore wind turbines*. Wiley.

Bienen, B., & Cassidy, M. J. 2006. Advances in the three-dimensional fluid–structure–soil interaction analysis of offshore jack-up structures. *Marine Structures*, 19(2-3), 110-140.

Byrne, B. W., & Houlsby, G. T. 2003. Foundations for offshore wind turbines. *Philosophical Transactions of the Royal Society of London. Series A: Mathematical, Physical and Engineering Sciences*, 361(1813), 2909-2930.

Byrne, B. W., Burd, H. J., Zdravkovic, L., Abadie, C. N., Houlsby, G. T., Jardine, R. J., ... & Potts, D. M. 2019. PISA Design Methods for Offshore Wind Turbine Monopiles. In *Offshore Technology Conference*. Offshore Technology Conference, Houston (USA).

Castro-Santos, L., & Diaz-Casas, V. (Eds.). (2016). Floating offshore wind farms. Springer.

Cerfontaine, B., Dieudonné, A. C., Radu, J. P., Collin, F., & Charlier, R. 2015. 3D zero-thickness coupled interface finite element: Formulation and application. *Computers and Geotechnics*, 69, 124-140.

Chong, S. H., & Pasten, C. 2018. Numerical study on long-term monopile foundation response. *Marine Georesources & Geotechnology*, 36(2), 190-196.

Corciulo, S., Zanoli, O., & Pisanò, F. 2017a. Transient response of offshore wind turbines on monopiles in sand: role of cyclic hydro–mechanical soil behaviour. *Computers and Geotechnics*, 83, 221-238.

Corciulo, S., Zanoli, O., & Pisanò, F. 2017b. Supporting the engineering analysis of offshore wind turbines through advanced soil-structure 3D modelling. In Proc. 36th Int. Conf. on Ocean, Offshore and Arctic Engineering (OMAE2017). June 25-30, 2017, Trondheim (Norway)

Corti, R., Diambra, A., Wood, D. M., Escribano, D. E., & Nash, D. F. 2016. Memory surface hardening model for granular soils under repeated loading conditions., 142(12), 04016102.

Cuéllar, P., Baeßler, M., & Rücker, W. 2009. Ratcheting convective cells of sand grains around offshore piles under cyclic lateral loads. *Granular Matter*, 11(6), 379.

Cuéllar, P., Mira, P., Pastor, M., Merodo, J. A. F., Baeßler, M., & Rücker, W. 2014. A numerical model for the transient analysis of offshore foundations under cyclic loading. *Computers and Geotechnics*, 59, 75-86.

Dafalias, Y. F., & Popov, E. P. 1975. A model of nonlinearly hardening materials for complex loading. *Acta mechanica*, 21(3), 173-192.

Dafalias, Y. F., & Manzari, M. T. 2004. Simple plasticity sand model accounting for fabric change effects. *Journal of Engineering mechanics*, 130(6), 622-634.

di Prisco, C., & Pisanò, F. 2011. Seismic response of rigid shallow footings. *European Journal of*

Environmental and Civil Engineering, 15(sup1), 185-221.

di Prisco, C. G., & Wood, D. M. (2012). *Mechanical Behaviour of Soils Under Environmentallly-Induced Cyclic Loads*. Springer Science & Business Media.

DNV-GL. 2016. Support structures for wind turbines - Standard DNV-GL-ST-0126. DNV-GL AS.

Doherty, P. & Gavin, K. 2011. Laterally loaded monopile design for offshore wind farms. Proceedings of the Institution of Civil Engineers, 165(EN1):7-17.

Elgamal, A., Yang, Z., Parra, E., & Ragheb, A. 2003. Modeling of cyclic mobility in saturated cohesionless soils. *International Journal of Plasticity*, 19(6), 883-905.

Ghofrani, A., & Arduino, P. 2018. Prediction of LEAP centrifuge test results using a pressure-dependent bounding surface constitutive model. *Soil Dynamics and Earthquake Engineering*, 113, 758-770.

Graff, K. F. 1975. *Wave motion in elastic solids*. Oxford University Press.

Griffiths, D. V. 1985. Numerical modelling of interfaces using conventional finite elements. In *Proc. of the 5th Int. Con on Numerical Methods in Geomechanics*, Nagoya (Japan).

Houlsby, G. T., & Puzrin, A. M. 2007. *Principles of hyperplasticity: an approach to plasticity theory based on thermodynamic principles*. Springer Science & Business Media.

Houlsby, G. T. 2016. Interactions in offshore foundation design. *Géotechnique*, 66(10), 791-825.

Houlsby, G. T., Abadie, C. N., Beuckelaers, W. J. A. P., & Byrne, B. W. 2017. A model for nonlinear hysteretic and ratcheting behaviour. *International Journal of Solids and Structures*, 120, 67-80.

Hughes, T. J. 1987. *The Finite Element Method: linear static and dynamic finite element analysis.* Prentice-Hall.

Jacobson, M. Z., Delucchi, M. A., Bazouin, G., Bauer, Z. A., Heavey, C. C., Fisher, E., ... & Yeskoo, T. W. 2015. 100% clean and renewable wind, water, and sunlight (WWS) all-sector energy roadmaps for the 50 United States. *Energy & Environmental Science*, 8(7), 2093-2117.

Jeng, D. S. 2003. Wave-induced sea floor dynamics. *Applied Mechanics Reviews*, 56(4), 407-429.

Jeremić, B., Cheng, Z., Taiebat, M., & Dafalias, Y. 2008. Numerical simulation of fully saturated porous materials. *International Journal for Numerical and Analytical Methods in Geomechanics*, 32(13), 1635-1660.

Jostad, H. P., Grimstad, G., Andersen, K. H., Saue, M., Shin, Y., & You, D. 2014. A FE procedure for foundation design of offshore structures–applied to study a potential OWT monopile foundation in the Korean Western Sea. *Geotechnical Engineering Journal of the SEAGS & AGSSEA*, 45(4), 63-72.

Kallehave, D., Thilsted, C. L., & Liingaard, M. A. 2012. Modification of the API py formulation of initial stiffness of sand. In *Offshore site investigation and geotechnics: integrated technologies-present and future*. Society of Underwater Technology.

Kallehave, D., Byrne, B. W., LeBlanc Thilsted, C., & Mikkelsen, K. K. 2015. Optimization of monopiles for offshore wind turbines. *Philosophical Transactions of the Royal Society A: Mathematical, Physical and Engineering Sciences*, 373(2035), 20140100.

Kaynia, A. M. (2018). Seismic considerations in design of offshore wind turbines. *Soil Dynamics and Earthquake Engineering*. DOI: 10.1016/j.soildyn.2018.04.038

Kementzetzidis, E., Versteijlen, W. G., Nernheim, A., & Pisanò, F. 2018. 3D FE dynamic modelling of offshore wind turbines in sand: natural frequency evolution in the pre–to after-storm transition. In *Proc. 9th European Conf. on Numerical Methods in Geotechnical Engineering (NUMGE 2018)*, June 25-27, 2018, Porto (Portugal).

Kementzetzidis, E., Corciulo, S., Versteijlen, W. G., & Pisanò, F. 2019a. Geotechnical aspects of offshore wind turbine dynamics from 3D non-linear soil-structure simulations. *Soil Dynamics and Earthquake Engineering*, 120, 181-199.

Kementzetzidis, E., Metrikine, A. V., Versteijlen, W. G., & Pisanò, F. 2019b. Frequency effects in the dynamic lateral stiffness of monopiles in sand: insight from field tests and 3D FE modelling. Under Review.

Kontoe, S., Zdravkovic, L., & Potts, D. M. 2008. An assessment of time integration schemes for

dynamic geotechnical problems. *Computers and Geotechnics*, 35(2), 253-264.

Kramer, S. L., Sideras, S. S., & Greenfield, M. W. 2016. The timing of liquefaction and its utility in liquefaction hazard evaluation. *Soil Dynamics and Earthquake Engineering*, 91, 133-146.

Kuo, Y. S., Achmus, M., & Abdel-Rahman, K. 2011. Minimum embedded length of cyclic horizontally loaded monopiles. *Journal of Geotechnical and Geoenvironmental Engineering*, 138(3), 357-363.

LeBlanc, C., Houlsby, G. T., & Byrne, B. W. 2010. Response of stiff piles in sand to long-term cyclic lateral loading. *Géotechnique*, 60(2), 79-90.

Li, W., Igoe, D., & Gavin, K. 2015. Field tests to investigate the cyclic response of monopiles in sand. *Proceedings of the Institution of Civil Engineers-Geotechnical Engineering*, 168(5), 407-421.

Li, Q., Prendergast, L. J., Askarinejad, A., & Gavin, K. 2018. Effect of scour on the behavior of a combined loaded monopile in sand. In *Proc. 9th European Conf. on Numerical Methods in Geotechnical Engineering (NUMGE 2018)*, June 25-27, 2018, Porto (Portugal).

Li, Z., Kotronis, P., Escoffier, S., & Tamagnini, C. 2016. A hypoplastic macroelement for single vertical piles in sand subject to three-dimensional loading conditions. *Acta Geotechnica*, 11(2), 373-390.

Liu, H. Y., Abell, J. A., Diambra, A., & Pisanò, F. 2018a. Modelling the cyclic ratcheting of sands through memory-enhanced bounding surface plasticity. *Géotechnique*, 1-18. DOI: 10.1680/jgeot.17.P.307

Liu, H. Y., Zygounas, F., Diambra, A., & Pisanò, F. 2018b. Enhanced plasticity modelling of high-cyclic ratcheting and pore pressure accumulation in sands. In *Proc. 9th European Conf. on Numerical Methods in Geotechnical Engineering (NUMGE 2018)*, June 25-27, 2018, Porto (Portugal).

Liu, H. Y., & Pisanò, F. 2019a. Prediction of oedometer terminal densities through a memory-enhanced cyclic model for sand. *Géotechnique Letters*, 9(2), 1-8.

Liu, H. Y., Abell, J. A., Diambra, A., & Pisanò, F. 2019b. Capturing cyclic mobility and preloading effects in sand using a memory-surface hardening model. In *Proc. of 7th Int. Conf. on Earthquake Geotechnical Engineering (7ICEGE)*, June 17-20, 2019, Rome (Italy).

Liu, H. Y., Diambra, A., Abell, J. A., & Pisanò, F. 2019c. Memory-enhanced plasticity modelling of sand behaviour under undrained cyclic loading. Under review.

Liu, H. Y. 2020. *Constitutive modelling of cyclic sand behaviour for offshore foundations*. PhD Thesis, Delft University of Technology.

Manzari, M. T., & Dafalias, Y. F. 1997. A critical state two-surface plasticity model for sands. *Géotechnique*, 47(2), 255-272.

Mazzoni, S., McKenna, F., Scott, M, & Fenves, G. 2007. *OpenSees command language manual*.

Mašín, D. 2018. *Modelling of Soil Behaviour with Hypoplasticity: Another Approach to Soil Constitutive Modelling*. Springer.

McGann, C. R., Arduino, P., & Mackenzie-Helnwein, P. 2015. A stabilized single-point finite element formulation for three-dimensional dynamic analysis of saturated soils. *Computers and Geotechnics*, 66, 126-141.

McKenna, F. T. 1997. *Object-oriented finite element programming: frameworks for analysis, algorithms and parallel computing*. Ph.D. Thesis, University of California Berkeley.

Miner, M. 1945. Cumulative damage in fatigue. *Transactions of the American Society of Mechanical Engineering*, 67:A159–64.

Mroz, Z. 1967. On the description of anisotropic workhardening. *Journal of the Mechanics and Physics of Solids*, 15(3), 163-175.

Muir Wood, D., Belkheir, K., & Liu, D. 1994. Strain softening and state parameter for sand modelling. *Géotechnique*, 44(2), 335-339.

Newman, J. N. 1977. *Marine hydrodynamics*. MIT press.

Nicolai, G., Ibsen, L. B., O'Loughlin, C. D., & White, D. J. 2017. Quantifying the increase in lateral capacity of monopiles in sand due to cyclic loading. *Géotechnique Letters*, 7(3), 245-252.

Niemunis, A., Wichtmann, T., & Triantafyllidis, T. 2005. A high-cycle accumulation model for sand. *Computers and Geotechnics*, 32(4), 245-263.

Nova, R., & Montrasio, L. (1991). Settlements of shallow foundations on sand. *Géotechnique*, 41(2), 243-256.

Page, A. M., Grimstad, G., Eiksund, G. R., & Jostad, H. P. 2019a. A macro-element model for multidirectional cyclic lateral loading of monopiles in clay. *Computers and Geotechnics*, 106, 314-326.

Page, A. M., Næss, V., De Vaal, J. B., Eiksund, G. R., & Nygaard, T. A. 2019b. Impact of foundation modelling in offshore wind turbines: Comparison between simulations and field data. *Marine Structures*, 64, 379-400.

Papadimitriou, A. G., Bouckovalas, G. D., & Dafalias, Y. F. 2001. Plasticity model for sand under small and large cyclic strains. *Journal of Geotechnical and Geoenvironmental Engineering*, 127(11), 973-983.

Park, J., & Santamarina, J. C. 2018. Sand response to a large number of loading cycles under zero-lateral-strain conditions: evolution of void ratio and small-strain stiffness. *Géotechnique*, 1-13.

Petalas, A. L., Dafalias, Y. F., & Papadimitriou, A. G. 2019. SANISAND-FN: An evolving fabric-based sand model accounting for stress principal axes rotation. *International Journal for Numerical and Analytical Methods in Geomechanics*, 43(1), 97-123.

Pisanò, F., di Prisco, C. G., & Lancellotta, R. 2014. Soil-foundation modelling in laterally loaded historical towers. *Géotechnique*, 64(1), 1.

Pisanò, F., & Gavin, K. G. 2017. General report for TC209 – Offshore Geotechnics, In *Proc. 19th Int. Conf. on Soil Mechanics and Geotechnical Engineering (ICSMGE 2017)*, September 17-22, 2017, Seoul (South Korea)

Pisanò, F., Schipper, R., & Schreppers, G. J. 2019. Input of fully 3D FE soil-structure modelling to the operational analysis of jack-up structures. *Marine Structures*, 63, 269-288.

Prendergast, L. J., Gavin, K., & Doherty, P. 2015. An investigation into the effect of scour on the natural frequency of an offshore wind turbine. *Ocean Engineering*, 101, 1-11.

Prévost, J. H. 1982. Two-surface versus multi-surface plasticity theories: a critical assessment. *International Journal for Numerical and Analytical Methods in Geomechanics*, 6(3), 323-338.

Prévost, J. H., & Popescu, R. 1996. Constitutive relations for soil materials. *Electronic journal of geotechnical engineering*, 1.

Rodrigues, S., Restrepo, C., Kontos, E., Pinto, R. T., & Bauer, P. (2015). Trends of offshore wind projects. *Renewable and Sustainable Energy Reviews*, 49, 1114-1135.

Rudolph, C., Bienen, B., & Grabe, J. 2014. Effect of variation of the loading direction on the displacement accumulation of large-diameter piles under cyclic lateral loading in sand. *Canadian Geotechnical Journal*, 51(10), 1196-1206.

Schotman, G. J. M. 1989. The effects of displacements on the stability of jackup spud-can foundations. In *Offshore Technology Conference*. Offshore Technology Conference.

Sloan, S. W. 1987. Substepping schemes for the numerical integration of elastoplastic stress–strain relations. *International Journal for Numerical Methods in Engineering*, 24(5), 893-911.

Staubach, P., & Machacek, J. 2019. Influence of relative acceleration in saturated sand: analytical approach and simulation of vibratory pile driving tests. *Computers and Geotechnics*,112, 173-184

Stockwell, R. G., Mansinha, L., & Lowe, R. P. 1996. Localization of the complex spectrum: the S transform. *IEEE transactions on signal processing*, 44(4), 998-1001.

Stutz, H., Mašín, D., Sattari, A. S., & Wuttke, F. 2017. A general approach to model interfaces using existing soil constitutive models application to hypoplasticity. *Computers and Geotechnics*, 87, 115-127.

Taiebat, M., & Dafalias, Y. F. 2008. SANISAND: Simple anisotropic sand plasticity model. *International Journal for Numerical and Analytical Methods in Geomechanics*, 32(8), 915-948.

Tamagnini, C., Viggiani, G., Chambon, R., & Desrues, J. 2000. Evaluation of different strategies for the integration of hypoplastic constitutive equations: Application to the CLoE model. *Mechanics of Cohesive frictional Materials*, 5(4), 263-289.

Truong, P., Lehane, B. M., Zania, V., & Klinkvort, R. T. 2018. Empirical approach based on centrifuge testing for cyclic deformations of laterally loaded piles in sand. *Géotechnique*, 69(2), 133-145.

Ushiyama, I. (2018). Present status and target of Japanese wind power generation. In *Transition Towards 100% Renewable Energy* (pp. 433-440). Springer, Cham.

van Kuik, G. A. M., Peinke, J., Nijssen, R., Lekou, D., Mann, J., Sørensen, J. N., ... & Polinder, H. 2016. Long-term research challenges in wind energy–a research agenda by the European Academy of Wind Energy. *Wind Energy Science*, 1(1), 1-39.

Vacareanu, V., Kementzetzidis, E., & Pisanò, F. 2019. 3D FE seismic analysis of a monopile-supported offshore wind turbine in a non-liquefiable soil deposit. In Proc. of 2nd Int. Conf. on Natural Hazards & Infrastructure (ICONHIC2019), 23-26 June 2019, Chania (Greece).

Versteijlen, W. G., Renting, F. W., van der Valk, P. L. C., Bongers, J., van Dalen, K. N., & Metrikine, A. V. 2017. Effective soil-stiffness validation: Shaker excitation of an in-situ monopile foundation. *Soil Dynamics and Earthquake Engineering*, 102, 241-262.

Watanabe, K., Pisanò, F., & Jeremić, B. 2017. Discretization effects in the finite element simulation of seismic waves in elastic and elastic-plastic media. *Engineering with Computers*, 33(3), 519-545.

Wichtmann, T. (2005). *Explicit accumulation model for non-cohesive soils under cyclic loading*. PhD thesis, Institut für Grundbau und Bodenmechanik, Bochum University.

Wichtmann, T., Niemunis, A., & Triantafyllidis, T. 2010. Strain accumulation in sand due to drained cyclic loading: on the effect of monotonic and cyclic preloading (Miner's rule). *Soil Dynamics and Earthquake Engineering*, 30(8), 736-745.

Wichtmann, T., Triantafyllidis, T., Chrisopoulos, S., & Zachert, H. 2017. Prediction of Long-Term Deformations of Offshore Wind Power Plant Foundations Using HCA-Based Engineer-Oriented Models. *International Journal of Offshore and Polar Engineering*, 27(04), 346-356.

Wichtmann, T., & Triantafyllidis, T. 2017. Strain accumulation due to packages of cycles with varying amplitude and/or average stress–On the bundling of cycles and the loss of the cyclic preloading memory. *Soil Dynamics and Earthquake Engineering*, 101, 250-263.

WindEurope. 2019. Offshore wind in Europe: key trends and statistics 2018. Via internet: *https://windeurope.org/about-wind/statistics/offshore/european-offshore-wind-industry-key-trends-statistics-2018/*.

Yang, Z. & Elgamal, A. 2008. Multi-surface cyclic plasticity sand model with Lode angle effect. *Geotechnical and Geological Engineering*, 26(3), 335-348.

Zhang, Y., Zhang, C., Chang, Y. C., Liu, W. H., & Zhang, Y. 2017. Offshore wind farm in marine spatial planning and the stakeholders engagement: opportunities and challenges for Taiwan. *Ocean & coastal management*, 149, 69-80.

Zienkiewicz, O. C., Chang, C. T., & Bettess, P. 1980. Drained, undrained, consolidating and dynamic behaviour assumptions in soils. *Géotechnique*, 30(4), 385-395.

Zienkiewicz, O. C., & Mroz, Z. 1984. Generalized plasticity formulation and applications to geomechanics. *Mechanics of engineering materials*, 44(3), 655-680.

Zienkiewicz, O. C., Chan, A. H. C., Pastor, M., Schrefler, B. A., & Shiomi, T. 1999. *Computational geomechanics*. Wiley.